Macromolecules

Article

pubs.acs.org/Macromolecules

The Origin of the Slow Mode in Dilute Aqueous Solutions of PEO

Jianqi Wang*

Department of Chemistry, The Chinese University of Hong Kong, Shatin, N.T., Hong Kong

ABSTRACT: Besides the fast translational diffusion of individual chains, a slow relaxation mode is frequently observed in dilute poly(ethylene oxide) (PEO) aqueous solutions in dynamic laser light scattering (LLS) experiments, which was attributed to some hydrophobic impurities in PEO or interchain association. Recently, we also encountered such a slow mode when studying dilute solutions of star-like PEO chains in water, hindering our further study of their dynamics in semidilute solutions. Using a combination of static and dynamic LLS, we found that the slow mode is removable after repeated filtration through a hydrophilic 0.45 μm PTFE filter or heating at 55 °C, resulting in a stable solution with only one fast translational mode of individual chains even after 5 months. Further, we found that an injection of a small amount of air regenerated the slow mode, revealing its origin, small air bubbles stabilized by the PEO chains adsorbed at the air/water interface, not previously proposed impurities or equilibrium between large interchain aggregates and individual chains. Our result has clarified a long-standing confusion of whether PEO is completely soluble in water as individual chains at room temperature. Our finding is important since aqueous solutions of PEO and its copolymers are widely used as model systems in academic research and as important ingredients in various industrial applications.

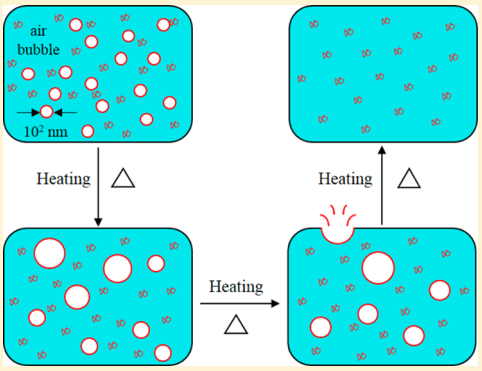

INTRODUCTION

Poly(ethylene oxide) (PEO) and its copolymers are widely used synthetic polymer materials in both academic research and industrial applications, especially as nonionic surfactant/stabilizer, due to their unique chemical and physical properties. They are commercially applied in cosmetics, foodstuffs, and pharmacy.[1] Besides polymer research, this moiety has also been extensively used in other fields, e.g., as a precipitant for isolation of plasmid DNA, an additive in crystallization of proteins, or a promoter to facilitate the cell fusion,[2] to name but a few. In recent biomedical and bioengineering applications, it is used to chemically modify protein and oligonucleotide due to its excellent biosafety and water solubility.[2−5] Therefore, solution behaviors of linear PEO and its copolymers, especially in aqueous solutions, have been studied and understood in the past.

Recently, we prepared 4-arm star-like PEO and tried to study their concentration dependent solution dynamics, covering from dilute to semidilute regimes, but were hindered by a repeatable/unexpected slow relaxation mode observed even in dilute PEO solutions in dynamic laser light scattering (LLS), as shown in Figure 1. PEO is a well-known water-soluble and neutral polymer and there should be no interchain association in dilute aqueous solutions. Literature search showed that such a slow mode in dilute linear PEO aqueous solutions was previously reported.[6−14] Very different from neutral polymers in organic solvents, such as polystyrene in cyclohexane, where the slow relaxation mode appears only when the polymer concentration is higher than the overlap concentration,[15−18] the slow relaxation mode persists in very dilute PEO aqueous solutions. How can one explain such an experimental observation? Some of previous studies attributed this slow mode to large PEO aggregates that are in equilibrium with individual chains because of its hydrophobic backbone moiety, $-CH_2-CH_2-$.[10,11] However, it is difficult to imagine how water-soluble PEO chains could associate with each other because its lower critical solution temperature is much higher than room temperature. This is why others suggested that the slow mode is due to the existence of a trace amount of hydrophobic impurities introduced during the sample preparation,[7,19−22] especially when the slow mode could be removed by careful filtration.[7,19,20] To the best of our knowledge, no consensus has been reached so far.[8]

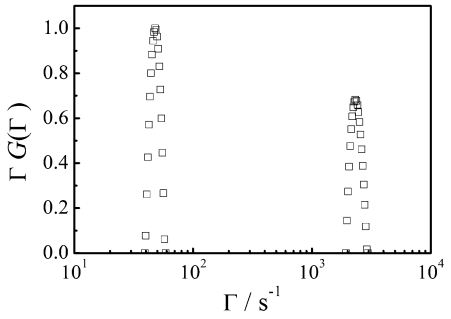

Figure 1. Characteristic line-width distribution of 4-arm star-like PEO in water, where $M_w = 9.9 \times 10^3$ g/mol, $T = 25$ °C, $C = 10$ mg/mL and $\theta = 20°$.

Received: November 20, 2014
Revised: February 13, 2015
Published: February 27, 2015

ACS Publications © 2015 American Chemical Society

DOI: 10.1021/ma5023428
Macromolecules 2015, 48, 1614−1620

It should be noted that we purified each PEO sample before LLS by precipitation in freshly distilled diethyl ether and further recrystallization in 2-propanol. However, the slow relaxation mode persists in dilute impurity-free PEO solutions. Therefore, we decided to figure out the true origin of the slow relaxation mode in the current study. Also note that a similar slow relaxation mode occurs in mixtures of water and a range of completely water-miscible organic solvents, including α-cyclodextrin and tetrahydrofuran.[23−26] It was demonstrated that the slow mode in α-cyclodextrin aqueous solutions could be removed by adding NaCl, just as that in PEO aqueous solutions.[11,24] Previously, a combination of LLS and isothermal compressibility measurements revealed that the slow mode was due to the spontaneous formation of small bubbles stabilized by those small water-soluble amphiphilic organic molecules, not of those suggested water/solute supramolecular structures.[23] The existence of small air bubbles (10^2 nm in size) was verified by different techniques, including direct scanning electron microscopy (SEM),[27] optic/fluorescence microscopy[28−30] or indirect nuclear magnetic resonance (NMR),[31] and total internal refractive microscopy (TIRM).[26] Since both α-cyclodextrin and PEO molecules have ether bonds, we thought that the slow mode observed in dilute PEO aqueous solutions might also be related to the formation of small air bubbles. This was our starting point in the current study.

EXPERIMENTAL SECTION

Materials. Four linear poly(ethylene oxide) (PEO) samples, respectively, with weight-average molar masses (M_w) of 2.0×10^3, 4.6×10^3, 8.0×10^3 and 1.0×10^4 g/mol were purchased from Sigma-Aldrich. Analytical grade dichloromethane, diethyl ether and 2-propanol were purchased from LAB-SCAN. Deionized water was freshly dispensed from Millipore Direct-Q 3 Ultrapure Water System with a resistivity of 18.2 MΩ·cm at 25 °C. Diethyl ether was purified by MBRAUN Solvent Purification Systems. To remove any possible hydrophobic inhibitor, PEO samples were first dissolved in dichloromethane, then precipitated in freshly dispensed diethyl ether, and finally dried in vacuum overnight. Each PEO sample was further recrystallized from isopropyl alcohol (IPA), washed with cold IPA and dried again in vacuum at 35 °C overnight.

Solution Preparation. The PEO aqueous solutions were gravimetrically prepared. After PEO was dissolved in deionized water, the solution was gently shaken and allowed to stand overnight in dark at room temperature. No stirring or ultrasonication was applied because the PEO chains might be cleaved by the shearing force, as shown by Duval et al.[11,32] To avoid any possible chain entanglement, the concentrations used were much lower than the overlap concentration (~70 mg/mL even for longest PEO chains used, assuming that the chain adopts a random coil conformation), ranging from 2 mg/mL to 20 mg/mL. For laser light scattering (LLS) experiments, dusts were removed from these aqueous solutions by one-time slow filtration using a normal syringe and a Millipore 0.45 μm PTFE hydrophilic filter, which *did not* remove the slow mode. After the LLS measurements, each solution was further repeatedly filtrated by using a tubing flex pump (Masterflex) and the same type of filter. In the repeated filtration, each solution was circulated to slowly pass through the filter and the LLS cuvette in a closed loop.

Laser Light Scattering. The commercial LLS spectrometer (ALV/DLS/SLS-5022F) equipped with a multi-τ digital time correlator (ALV5000) and a vertically polarized 22 mW He−Ne cylindrical laser (λ_0 = 632.8 nm, Uniphase) was used. The details of LLS instrumentation and theory can be found elsewhere.[33−35] In static LLS, the excess absolute time-averaged scattered light intensity at a given scattering vector q, known as the excess Rayleigh ratio $R_{vv}(q)$, of a dilute polymer solution at a concentration C (g/mL) is related to the weigh average molar mass (M_w), the root-mean square z-average radius of gyration ($\langle R_g^2\rangle_z^{1/2}$) (or written as $\langle R_g\rangle$), and the second virial coefficient (A_2) as

$$\frac{KC}{R_{vv}(q)} \approx \frac{1}{M_w}\left(1 + \frac{1}{3}\langle R_g^2\rangle q^2\right) + 2A_2C \tag{1}$$

where $K = 4\pi^2 n^2 (dn/dC)^2/(N_A\lambda_0^4)$ and $q = 4\pi n \sin(\theta/2)/\lambda_0$ with N_A, dn/dC, n, θ, and λ_0 being Avogadro's number, the specific refractive index increment, the solvent refractive index, the scattering angle, and the wavelength of the incident light in vacuum, respectively. When the polymer concentration is sufficiently low, the second term on the right side of eq 1 is droppable so that the plot of $[KC/R_{vv}(q)]$ versus q^2 can lead to both M_w and $\langle R_g\rangle$.

In dynamic LLS, the measured intensity−intensity time correlation function $G^{(2)}(q,t)$ is related to the normalized electric field−field time correlation function $g^{(1)}(q,t)$ by the Siegert relation as

$$G^{(2)}(q, t) = A[1 + \beta|g^{(1)}(q, t)|^2] \tag{2}$$

where A is the measured baseline and β is the coherent factor, depending on the detection optics. For a system with different relaxation modes, $|g^{(1)}(q,t)|$ is generally related to a characteristic line-width distribution $G(\Gamma, q)$ as

$$|g^{(1)}(q, t)| = \int G(\Gamma, q)e^{-\Gamma(q)t}\, d\Gamma \tag{3}$$

$G(\Gamma, q)$ can be obtained by the Laplace inversion of each measured $|G^{(2)}(q,t)|$ using the CONTIN program. In this study, only two narrowly distributed relaxation modes were observed so that we can rewrite $|g^{(1)}(q,t)|$ as a combination of two exponetials,[33] i.e.,

$$|g^{(1)}(q, t)| = A_{fast}(q)e^{-\Gamma_{fast}(q)t} + A_{slow}(q)e^{-\Gamma_{slow}(q)t} \tag{4}$$

where $A_{fast}(q)$ is the normalized intensity contribution of the fast mode and $A_{slow}(q) = 1 - A_{fast}(q)$ for the slow mode. For a pure diffusive relaxation, the plot of Γ verse q^2 is a straight line passing through the origin, with its slope as the average translational diffusion coefficient constant ($\langle D\rangle$) of the scattering objects. The hydrodynamic radius ($\langle R_h\rangle$) can be further calculated from $\langle D\rangle$ by using the Stokes−Einstein equation.

A combination of static and dynamic LLS results can lead to the excess scattered intensities related to the fast and slow modes, respectively; namely, $\langle \Delta I(q)\rangle_{fast} = A_{fast}(q)\langle \Delta I(q)\rangle_{total}$ and $\langle \Delta I(q)\rangle_{slow} = [1 - A_{fast}(q)]\langle \Delta I(q)\rangle_{total}$. The plot of $1/\langle \Delta I(q)\rangle_{fast}$ versus q^2 or $1/\langle \Delta I(q)\rangle_{slow}$ versus q^2 on the basis of eq 1 can result in $\langle R_g\rangle_{fast}$ or $\langle R_g\rangle_{slow}$. In the current study, $\langle R_g\rangle_{fast}$ of individual PEO chains are too small to be measured by LLS because $\langle \Delta I(q)\rangle_{fast}$ has no angular dependence.

RESULTS AND DISCUSSION

As a starting point, it is rather important to find the nature of the slow mode observed in the dilute PEO aqueous solutions. Note that in dynamic LLS, one measures the relaxation of a given system and the translational diffusion is only one of the possibilities that cause the relaxation. The slow mode constantly observed in semidilute polymer or dilute polyelectrolytes solutions has been assigned to various origins, such as the q-independent relaxation of a transient network,[36,37] the q^2-dependent translational diffusion of large aggregates,[38−40] and the internal motions of large transient chain clusters (q^3 dependent).[41−43]

Figure 2 shows the typical scattering vector (q^2) dependence of the average characteristic line-width of the fast and slow modes of a dilute PEO aqueous solution. Both plots of $\langle\Gamma\rangle$ vs q^2 are straight lines passing through the origin, indicating that both of them are diffusive. After confirming their diffusive nature, we can first obtain the average translational diffusion coefficients ($\langle D\rangle_{fast}$ and $\langle D\rangle_{slow}$) from the respective slopes and

DOI: 10.1021/ma5023428
Macromolecules 2015, 48, 1614−1620

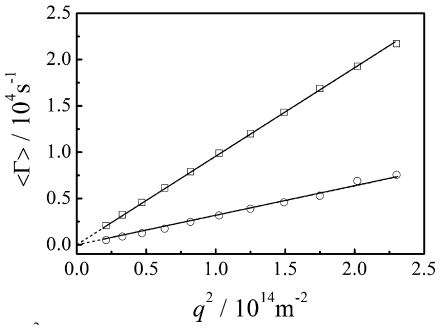

Figure 2. q^2-dependence of average characteristic line-width ($\langle\Gamma\rangle$) of fast (square) and slow mode (circle) of a dilute PEO aqueous solution, where $M_w = 1.0 \times 10^4$ g/mol, $C = 10$ mg/mL, $T = 25$ °C and $\langle\Gamma\rangle_{slow}$ is enlarged 10 times for better view.

then convert them to the average hydrodynamic radius ($\langle R_h\rangle$) using the Stokes–Einstein equation.

Figure 3 summarizes the chain-length dependence of the average hydrodynamic radii of the fast and slow modes. $\langle R_h\rangle_{fast}$

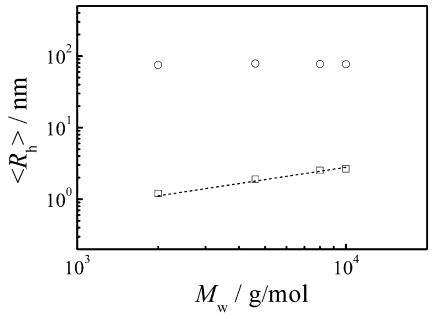

Figure 3. Molar mass dependence of average hydrodynamic radius ($\langle R_h\rangle_{fast}$ or $\langle R_h\rangle_{slow}$) related to fast (square) and slow modes (circle), where dash line represents $\langle R_h\rangle$ (nm) = $1.45 \times 10^{-2} M_w^{0.571}$ from ref 45.

increases with the chain length because it is related to the translational diffusion of individual PEO chains in the solutions.[44] A scaling of $\langle R_h\rangle$ (nm) = $1.45 \times 10^{-2} M_w^{0.571}$ was previously reported[45] and represented by the dash line here. The good agreement between our measured data and the scaling law confirms that the fast mode is related to the translational diffusion of individual PEO chains in the solutions. On the other hand, $\langle R_h\rangle_{slow}$ is essentially independent of the chain length.

Figure 4 shows how $\langle R_g\rangle_{slow}$ is obtained. The inset shows that $\langle R_g\rangle_{slow}$ and $\langle R_h\rangle_{slow}$ are independent of the PEO concentration and $\langle R_g\rangle_{slow}/\langle R_h\rangle_{slow} \sim 1$ over the entire concentration range investigated. It has been known that $\langle R_g\rangle/\langle R_h\rangle = 0.774$ for a uniform hard sphere;[46−48] $\langle R_g\rangle/\langle R_h\rangle = 1.5$ for linear and flexible polymer chains in good solvents;[33,49,50] and $\langle R_g\rangle/\langle R_h\rangle = 1$ for a hollow sphere with a very thin shell.[51−53] Therefore, our results indicate that the slow mode is related to diffusive objectives with a small hollow structure ($\sim 10^2$ nm), presumably, small air bubbles as we speculated because PEO is molecularly amphiphilic,[54] similar as small dioxane or THF molecules. Namely, PEO can act as a stabilizer to coalesce a trace amount of air molecules dissolved in water, also evidenced by the formation of a stable thin PEO monolayer at the air/water interface[55,56] and large bubbles during the preparation of PEO aqueous solutions.

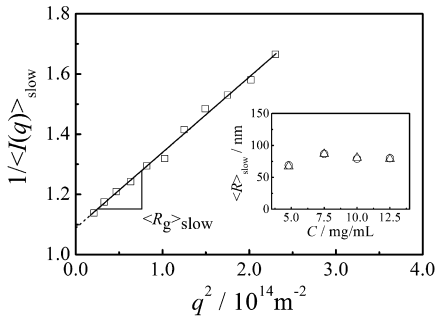

Figure 4. q^2-dependence of scattering intensity related to slow mode, where θ ranges from 20° to 70° to ensure $qR_g < 1$, slope of solid line leads to $\langle R_g\rangle_{slow}$ and inset shows concentration dependence of $\langle R_g\rangle_{slow}$ (circle) and $\langle R_h\rangle_{slow}$ (triangle), where $M_w = 1.0 \times 10^4$ g/mol, $T = 25$ °C, and $C = 7.5$ mg/mL.

The speculation of the slow mode is related to large PEO aggregates was examined by evaluating the molar mass of the scattering objects that are related to the slow mode. If the slow mode is related to the PEO aggregates as suggested previously, we would have[57]

$$M_{w,app} = M_{w,fast}x_{fast} + M_{w,slow}x_{slow} = M_{w,fast}x_{fast} + M_{w,slow}(1 - x_{fast}) \quad (5)$$

$$(A_r)_{q\to 0}^{C\to 0} = \left(\frac{A_{fast}}{A_{slow}}\right)_{q\to 0}^{C\to 0} = \frac{M_{w,fast}x_{fast}}{M_{w,slow}(1 - x_{fast})} \quad (6)$$

Here $M_{w,app}$ is the apparent weight-averaged molar mass calculated from the overall scattered light intensity, x is the weight fraction, and A_r is the area ratio of the two peaks in DLS that are respectively corresponding to the fast and slow modes. Duval et al.[10] passed a PEO aqueous solution repeatedly through a syringe needle to generate the slow mode and used eqs 5 and 6 to obtain $M_{w,slow} = 4.2 \times 10^4$ g/mol for the slow mode object with $\langle R_h\rangle = 77$ nm. Following the same calculation, we have $M_{w,slow} = 6.7 \times 10^4$ g/mol for the slow mode object with $\langle R_h\rangle \sim 10^2$ nm in the current study. Note that the PEO chains used in both cases have a weight-average molar mass of $\sim 10^4$ g/mol; namely, each aggregate would contain only few chains, which would not lead to scattering objects with a size of $\sim 10^2$ nm. Therefore, the slow mode cannot be related to large PEO chain aggregates.

On the other hand, assigning the slow mode to small air bubbles, we can estimate the weight concentration of those small air bubbles to be $\sim 10^{-9}$ g/mL from their scattering intensity because we can estimate their molar mass from their size and density. Note that here the scattered light is actually from small water droplets corresponding to small air bubbles with a phase difference of 180°. The air solubility in water is $\sim 10^{-5}$ g/mL at the standard condition. Therefore, only a very small amount of dissolved air is entrapped into small bubbles stabilized by the PEO chains at the air/water interface. This explains why we cannot remove these small air bubbles by the repeated freeze–pump–thaw cycles, as shown in Figures 5 and 6. Namely, the five repeated freeze–pump–thaw cycles have no obvious effect on the removal of the slow mode. The treatment is normally sufficient to remove gas in the solution in a living radical polymerization. The slight increase ($\sim$15%) of its related diffusion coefficient in Figure 6 reflects slight shrinking of small bubbles. The ineffective removal of small air bubbles by

DOI: 10.1021/ma5023428
Macromolecules 2015, 48, 1614−1620

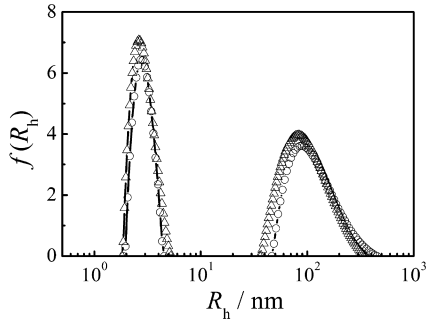

Figure 5. Hydrodynamic radius distributions of PEO aqueous solution before (circle) and after (triangle) five freeze–pump–thaw cycles, where $M_w = 1 \times 10^4$ g/mol, $C = 10$ mg/mL, $T = 25$ °C, and $\theta = 20°$.

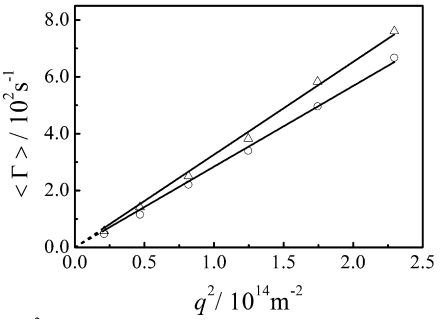

Figure 6. q^2 dependence of average line width of slow mode in PEO aqueous solution before (circle) and after (triangle) five freeze–pump–thaw cycles, where $M_w = 1 \times 10^4$ g/mol, $C = 10$ mg/mL, and $T = 25$ °C.

the freeze–pump–thaw cycle is also presumably due to the stabilization of PEO chains at the air/water interface. In the freezing process, the PEO chains vitrify to form a protective shell that prevents the rupture of those small bubbles.

The next question is how we can further prove that the slow mode is indeed related to small air bubbles formed inside water in the presence of PEO chains instead of previously suggested large interchain aggregates formed via the hydrophobic interaction among the chain backbones,[6,9−11,58] or hydrophobic impurities introduced during the polymer synthesis?[7,8,59] We noted that Jin et al.[23] previously developed a repeating extruding method to crash and remove small air bubbles inside aqueous solutions of water-soluble organic solvents by using a filter with 10^2-nm pores.

Figure 7 shows that the slow relaxation mode is indeed removable by the repeated filtration through a 0.45 μm PTFE hydrophilic filter. It is important to note that the repeated filtration has no effect on the fast relaxation mode; namely, no degradation of PEO chains was observed, different from previous observations that the PEO chains were broken under a strong shear force.[10,11] Such a discrepancy is attributed to different PEO chain lengths used; namely, much shorter PEO chains were used in the current study. Shorter chains relax much faster so that the chain relaxation time is much shorter than the chain stretching time under the filtration-generated shearing force. Also note that the filter used has pores with a size six times larger than $\langle R_g \rangle_{slow}$. If the slow relaxation mode was due to some hydrophobic impurities, the filtration would not be able to remove them. Here the filtration breaks small air bubbles or make them merge together.

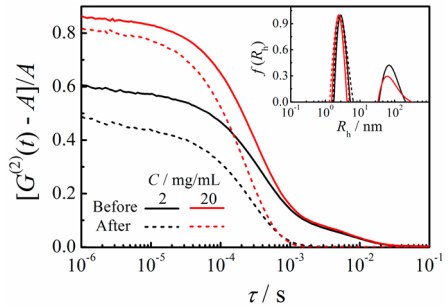

Figure 7. Effect of repeated filtration on normalized intensity–intensity time correlation function of PEO aqueous solutions with two different concentrations, where inset shows their corresponding hydrodynamic radius distributions $f(R_h)$, $M_w = 1.0 \times 10^4$ g/mol, $\theta = 20°$, $T = 25$ °C.

It is worth noting that the slow-mode-free PEO solution with only the remaining fast mode is extremely stable, as shown in Figure 8. There is no change in either the hydrodynamic radius

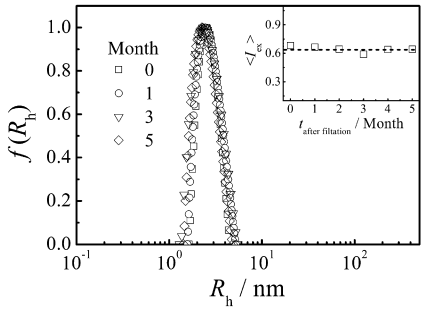

Figure 8. Time dependence of hydrodynamic radius distribution $f(R_h)$ of a PEO aqueous solution after repeated filtration to remove small air bubbles, where $M_w = 1.0 \times 10^4$ g/mol, $\theta = 20°$, $C = 10$ mg/mL, $T = 25$ °C, and the inset shows standing time dependence of corresponding normalized excess total scattering intensity $\langle I_{ex} \rangle$ after repeated filtration.

distribution or the scattered light intensity even after five months, completely ruling out a possible equilibrium between individual chains and large interchain aggregates. A similar result was also reported before by Porsch et al.,[7] where they did not do repeated filtration but used a membrane with much smaller 20 nm pores and much longer PEO chains ($M_w = 1.5 \times 10^5$ g/mol). After excluding possibilities of attributing the slow mode to some hydrophobic impurities or interchain association, we further tested whether the slow mode is indeed related to small air bubbles by purging a small amount of air into the repeated filtered slow-mode-free solution to see whether the slow relaxation mode can be regenerated.

Figure 9 shows that the air purge indeed regenerates the slow mode after it is removed by repeated filtration, supporting our speculation that the origin of the slow mode is the existence of small diffusive air bubbles in the PEO aqueous solutions. It is worth noting that the excess scattering intensity of the fast mode remains a constant during the filtration–purge cycle, indicating no change in both the length and concentration of individual PEO chains because the number of the PEO chains adsorbed at the air/water interface of small air bubbles is extremely small. Figure 9 also shows that the fast mode remains its position during the entire filtration–purging cycle, further indicating that the repeated filtration has no effect on the chain

DOI: 10.1021/ma5023428
Macromolecules 2015, 48, 1614−1620

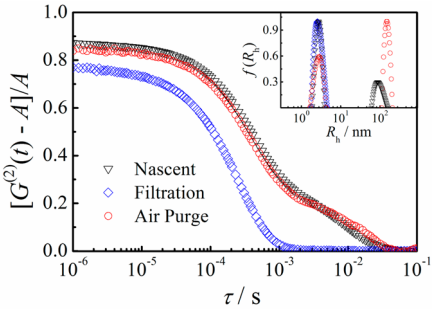

Figure 9. Effects of repeated filtration and air purge on the normalized intensity−intensity time correlation function of a PEO aqueous solution, where M_w = 1.0 × 10^4 g/mol, θ = 20°, C = 10 mg/mL, T = 25 °C, and the inset shows the corresponding hydrodynamic radius distributions $f(R_h)$.

length. At this point, we are confident to say that the slow mode observed in our PEO aqueous solutions is indeed originated from small air bubbles, not due to some hydrophobic impurities or large interchain aggregates. Namely, a trace amount of air is inevitably dissolved in water. The molecularly amphiphilic PEO chains pull those soluble air molecules (mostly N_2 and O_2) together to form small bubbles by adsorbing at the air/water interface to reduce the total surface energy.[23] To further confirm the air bubble origin, we heated the solutions to a higher temperature because the heating can make the air bubbles expand so that their stability decreases.

Figure 10 shows that after a temperature jump from 25 to 55 °C, both the normalized excess total scattering intensity and the

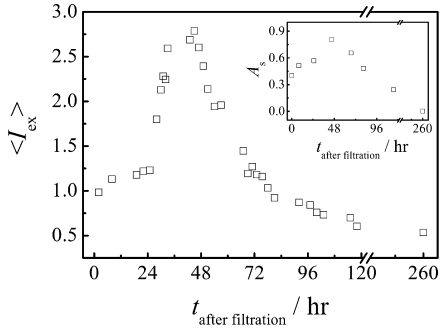

Figure 10. Time dependence of normalized excess scattering intensity after temperature jump from 25 to 55 °C, where M_w = 1.0 × 10^4 g/mol, θ = 20°, and C = 10 mg/mL. The inset shows the relative intensity contribution of slow mode.

intensity contribution of the slow mode first increase and reach their respective maxima after ∼2 days, and then, decrease and level off to their respective plateau values after ∼11 days. The similar heating effect was observed before but attributed to the dissolution of large interchain aggregates and the melting of residual PEO crystals.[10,11,60] Note that previous studies focused only on the change of the slow mode in dynamic LLS and overlooked the change of the scattering intensity. In principle, the dissolution of large interchain aggregates would lead to a gradual decrease of the scattering intensity until all the interchain aggregates become individual chains, contradicting to what we observed here.

Figure 10 can be well explained when we relate the slow mode to small air bubbles inside the PEO solutions. Heating the solution from 25 to 55 °C has two following effects. On one hand, the inner pressure of each bubble increases; and on the other hand, water becomes a less good solvent for PEO at higher temperatures so that the PEO chains are less swollen in water and their stabilization ability decreases. A combination of these two effects leads to expansion and coalescence of small air bubbles into larger ones, explaining why the scattering intensity initially increases because the excess scattering intensity is proportional to the square of the mass of a scattering object or the sixth power of its size if it is uniform. Such expansion and coalescence of small air bubbles is evidenced from the appearance of an additional slow relaxation mode located at ∼10 μm, as shown in Figure 11.

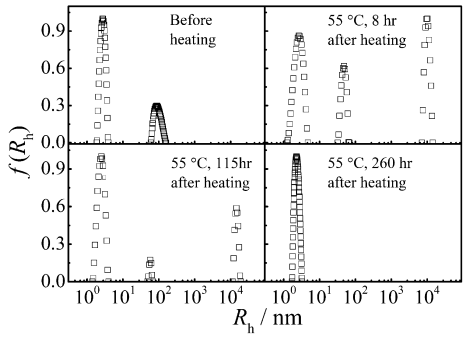

Figure 11. Effect of heating on hydrodynamic radius distribution of a PEO aqueous solution after a temperature jump from 25 to 55 °C, where M_w = 1.0 × 10^4 g/mol, θ = 20°, C = 10 mg/mL.

As the expansion and coalescence proceed, air bubbles change from the nanobubbles to the microbubbles and finally the macro-bubbles, floating upward and bursting at the air/solution surface, i.e., the turning point at ∼45 h. Note that only the fast mode related to translational diffusion of individual PEO chains remains after ∼11 days, indicating that air bubbles initially trapped in the solution have been dispelled. The heating effect is schematically shown in Figure 12.

Figure 13 shows that the heating resulted slow-mode-free PEO solution is very stable at room temperature even after one month, exactly like the repeated filtration resulted slow-mode-free solutions. A combination of Figures 11 and 13 further shows that the slow mode in dilute PEO aqueous solutions is

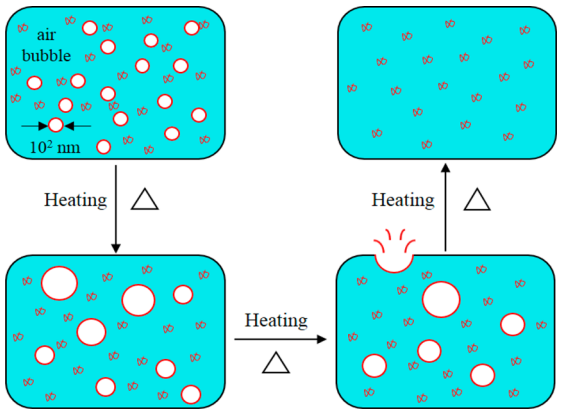

Figure 12. Schematic of heating effect on small air bubbles trapped in an aqueous solution of individual PEO chains (small twisted red lines), where cyan background represents water, and white spheres, which represent small air bubbles stabilized by amphiphilic PEO chains (red circles) absorbed at air/water interface.

DOI: 10.1021/ma5023428
Macromolecules 2015, 48, 1614−1620

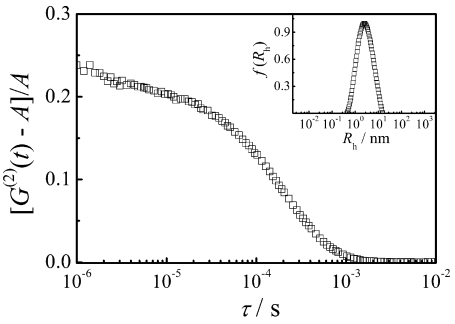

Figure 13. Normalized correlation function of a PEO aqueous solution at room temperature for one month after it was heated at 55 °C for 11 days, where $M_w = 1.0 \times 10^4$ g/mol, $\theta = 20°$, $C = 10$ mg/mL, and the inset shows the corresponding correlation function from CONTIN analysis.

not originated from possible hydrophobic interaction induced interchain aggregates or hydrophobic impurities introduced during the polymer synthesis. The current experimental evidence all points the slow relaxation mode to the formation of small air bubbles inside the PEO aqueous solutions, also directly/indirectly supported by some of previous studies.

For example, Duval et al.[11] found that the ultrasonic irradiation regenerated the slow mode in a heating-treated slow-mode-free aqueous solution of short PEO chains because it is well-known that the ultrasonic irradiation generates small cavities inside a liquid.[61−64] Successful confinement and stabilization of acoustically generated cavities has been realized with amphiphilic protein chains, evidenced by both scanning electron and fluorescence optical microscopic methods.[28] In addition, Kinugasa et al.[60] found that rapid filtration frequently led to an apparent upturn of the scattered light intensity, which can be attributed to the formation of small bubbles generated by a pressure difference in the rapid filtration process.[10] Moreover, it is well-known that adding electrolytes, such as NaCl, eliminates the slow mode.[10] The effect of salt concentration on the stability of small air bubbles was addressed by Jin et al.[24] Namely, small air bubbles are stabilized by the absorption of a layer of amphiphilic molecules at the air/water interface so that the interface has a layer of negatively charged OH^- ions. An increase of ionic strength reduces the double-layer thickness and increases the surface tension, destabilizing the small air bubbles.

CONCLUSION

A combination of static and dynamic LLS enables us to confirm that the slow relaxation mode, frequently appearing in the dilute aqueous solutions of poly(ethylene oxide) (PEO), is originated from small air bubbles that are formed and stabilized by the molecularly amphiphilic PEO chains absorbed at the air/water interface, not from some hydrophobic impurities introduced in the sample preparation or possible equilibrium between individual PEO chains and large interchain aggregates formed via hydrophobic interaction among the chain backbones. We have answered a long-standing controversial question and ascertain that PEO is completely soluble in water at room temperature. However, we do not rule out the possibility that some of the previous observation of the slow mode in some PEO aqueous solutions was due to hydrophobic impurities or interchain association. The present study demonstrates that special attention should be paid each time when we deal with aqueous solutions of water-soluble polymers that are molecularly amphiphilic in nature.

AUTHOR INFORMATION

Corresponding Author

*(J.W.) E-mail: agathis.wang@gmail.com.

Notes

The authors declare no competing financial interest.

ACKNOWLEDGMENTS

We thank Professor Chi Wu for pointing out small air bubbles as a possible origin of the slow mode in the dilute PEO aqueous solutions and for his help in the manuscript preparation. Financial support of the National Natural Scientific Foundation of China Projects (51173177 and 51273091), the Ministry of Science and Technology of China Key Project (2012CB933802), and the Hong Kong Special Administration Region Earmarked Projects (CUHK4035/12P, 2130306 and 4053005; CUHK4042/13P, 2130349 and 4053060; and CUHK7/CRF/12G, 2390062) is gratefully acknowledged.

REFERENCES

(1) Bailey, F. J.; Koleske, J. V. *Poly(ethylene oxide)*; Academic Press: New York, 1976.
(2) Harris, J. M.; Zalipsky, S. *Poly(ethylene glycol): Chemistry and Biological Applications*; American Chemical Society: Washington, DC, 1997.
(3) Drury, J. L.; Mooney, D. J. *Biomaterials* **2003**, *24*, 4337.
(4) Banerjee, I.; Pangule, R. C.; Kane, R. S. *Adv. Mater.* **2011**, *23*, 690.
(5) Veronese, F. M. *Biomaterials* **2001**, *22*, 405.
(6) Brown, W. *Polymer* **1985**, *26*, 1647.
(7) Porsch, B.; Sundeloef, L. O. *Macromolecules* **1995**, *28*, 7165.
(8) Sandier, A.; Brown, W.; Mays, H.; Amiel, C. *Langmuir* **2000**, *16*, 1634.
(9) Ho, D. L.; Hammouda, B.; Kline, S. R. *J. Polym. Sci., Part B: Polym. Phys.* **2003**, *41*, 135.
(10) Duval, M.; Boué, F. *Macromolecules* **2007**, *40*, 8384.
(11) Duval, M.; Gross, E. *Macromolecules* **2013**, *46*, 4972.
(12) Sakai, T.; Matsunaga, T.; Yamamoto, Y.; Ito, C.; Yoshida, R.; Suzuki, S.; Sasaki, N.; Shibayama, M.; Chung, U. I. *Macromolecules* **2008**, *41*, 5379.
(13) Layec, Y.; Layec-Raphalen, M.-N. *J. Phys. Lett. (Paris)* **1983**, *44*, 121.
(14) Polik, W. F.; Burchard, W. *Macromolecules* **1983**, *16*, 978.
(15) Li, J. F.; Li, W.; Huo, H.; Luo, S. Z.; Wu, C. *Macromolecules* **2008**, *41*, 901.
(16) Brown, W. *Macromolecules* **1984**, *17*, 66.
(17) Hwang, D. H.; Cohen, C. *Macromolecules* **1984**, *17*, 1679.
(18) Stepanek, P.; Brown, W. *Macromolecules* **1998**, *31*, 1889.
(19) Zhou, Z.; Chu, B. *Macromolecules* **1987**, *20*, 3089.
(20) Zhou, Z.; Chu, B. *Macromolecules* **1988**, *21*, 2548.
(21) Zhou, Z.; Chu, B. *Macromolecules* **1994**, *27*, 2025.
(22) Zhou, Z.; Chu, B. *J. Colloid Interface Sci.* **1988**, *126*, 171.
(23) Jin, F.; Ye, J.; Hong, L. Z.; Lam, H. F.; Wu, C. *J. Phys. Chem. B* **2007**, *111*, 2255.
(24) Jin, F.; Li, J.; Ye, X.; Wu, C. *J. Phys. Chem. B* **2007**, *111*, 11745.
(25) Jin, F.; Ye, X.; Wu, C. *J. Phys. Chem. B* **2007**, *111*, 13143.
(26) Jin, F.; Gong, X.; Ye, J.; Ngai, T. *Soft Matter* **2008**, *4*, 968.
(27) Ohgaki, K.; Khanh, N. Q.; Joden, Y.; Tsuji, A.; Nakagawa, T. *Chem. Eng. Sci.* **2010**, *65*, 1296.
(28) Zhou, M.; Cavalieri, F.; Caruso, F.; Ashokkumar, M. *ACS Macro Lett.* **2012**, *1*, 853.
(29) Chan, C. U.; Ohl, C.-D. *Phys. Rev. Lett.* **2012**, *109*, 174501.
(30) Karpitschka, S.; Dietrich, E.; Seddon, J. R. T.; Zandvliet, H. J. W.; Lohse, D.; Riegler, H. *Phys. Rev. Lett.* **2012**, *109*, 066102.
(31) Demangeat, J.-L. *J. Mol. Liq.* **2009**, *144*, 32.

DOI: 10.1021/ma5023428
Macromolecules 2015, 48, 1614−1620

(32) Duval, M.; Sarazin, D. *Macromolecules* **2003**, *36*, 1318.
(33) Chu, B. *Laser Light Scattering: Basic Principles and Practice*; Academic Press: San Diego, CA, 1991.
(34) Teraoka, I. *Polymer Solutions: An Introduction to Physical Properties*; Wiley: New York, 2002.
(35) Berne, B. J.; Pecora, R. *Dynamic light scattering: with applications to chemistry, biology, and physics*; Courier Dover Publications: Mineola, NY, 2000.
(36) Adam, M.; Delsanti, M. *Macromolecules* **1985**, *18*, 1760.
(37) Adam, M.; Delsanti, M. *Macromolecules* **1977**, *10*, 1229.
(38) Brown, W.; Stepanek, P. *Macromolecules* **1988**, *21*, 1791.
(39) Brown, W.; Stepanek, P. *Macromolecules* **1992**, *25*, 4359.
(40) Brown, W.; Stepanek, P. *Macromolecules* **1993**, *26*, 6884.
(41) Li, J.; Ngai, T.; Wu, C. *Polym. J.* **2010**, *42*, 609.
(42) Chu, B.; Nose, T. *Macromolecules* **1980**, *13*, 122.
(43) Ngai, T.; Wu, C. *Macromolecules* **2003**, *36*, 848.
(44) Duval, M.; Sarazin, D. *Polymer* **2000**, *41*, 2711.
(45) Devanand, K.; Selser, J. C. *Macromolecules* **1991**, *24*, 5943.
(46) Zhang, G.; Wu, C. *Adv. Polym. Sci.* **2006**, *195*, 101.
(47) Burchard, W.; Schmidt, M.; Stockmayer, W. H. *Macromolecules* **1980**, *13*, 1265.
(48) Antonietti, M.; Heinz, S.; Schmidt, M.; Rosenauer, C. *Macromolecules* **1994**, *27*, 3276.
(49) Wu, C.; Zhou, S. *Macromolecules* **1996**, *29*, 1574.
(50) Wu, C.; Zhou, S. *Phys. Rev. Lett.* **1996**, *77*, 3053.
(51) Schartl, W. *Light Scattering from Polymer Solutions and Nanoparticle Dispersions*; Springer: Berlin, 2007.
(52) Kim, D.; Kim, E.; Lee, J.; Hong, S.; Sung, W.; Lim, N.; Park, C. G.; Kim, K. *J. Am. Chem. Soc.* **2010**, *132*, 9908.
(53) Zhang, Y.; Guan, Y.; Zhou, S. *Biomacromolecules* **2005**, *6*, 2365.
(54) Israelachvili, J. *Proc. Natl. Acad. Sci. U.S.A.* **1997**, *94*, 8378.
(55) Glass, J. E. *J. Phys. Chem.* **1968**, *72*, 4459.
(56) Glass, J. E. *J. Polym. Sci., Polym. Symp.* **1971**, *34*, 141.
(57) Wu, C.; Siddiq, M.; Woo, K. F. *Macromolecules* **1995**, *28*, 4914.
(58) Hammouda, B. *Polymer* **2009**, *50*, 5293.
(59) Devanand, K.; Selser, J. *Nature* **1990**, *343*, 739.
(60) Kinugasa, S.; Nakahara, H.; Fudagawa, N.; Koga, Y. *Macromolecules* **1994**, *27*, 6889.
(61) Flint, E. B.; Suslick, K. S. *Science* **1991**, *253*, 1397.
(62) Caruso, M. M.; Davis, D. A.; Shen, Q.; Odom, S. A.; Sottos, N. R.; White, S. R.; Moore, J. S. *Chem. Rev.* **2009**, *109*, 5755.
(63) Suslick, K. S.; Price, G. J. *Annu. Rev. Mater. Sci.* **1999**, *29*, 295.
(64) Kuijpers, M. W. A.; van Eck, D.; Kemmere, M. F.; Keurentjes, J. T. F. *Science* **2002**, *298*, 1969.

DOI: 10.1021/ma5023428
Macromolecules 2015, 48, 1614−1620